

# A 490 GHz planar circuit balanced Nb-Al<sub>2</sub>O<sub>3</sub>-Nb quasiparticle mixer for radio astronomy: Application to quantitative local oscillator noise determination

M. P. Westig,<sup>a)</sup> M. Justen, K. Jacobs, J. Stutzki, M. Schultz, F. Schomacker, and C. E. Honingh  
*Kölner Observatorium für Submillimeter Astronomie (KOSMA), I. Physikalisches Institut, Universität zu Köln,  
 D-50937 Köln, Germany*

(Dated: 6 November 2018)

This article presents a heterodyne experiment which uses a 380-520 GHz planar circuit balanced Nb-Al<sub>2</sub>O<sub>3</sub>-Nb superconductor-insulator-superconductor (SIS) quasiparticle mixer with 4-8 GHz instantaneous intermediate frequency (IF) bandwidth to quantitatively determine local oscillator (LO) noise. A balanced mixer is a unique tool to separate noise at the mixer's LO port from other noise sources. This is not possible in single-ended mixers. The antisymmetric IV characteristic of a SIS mixer further helps to simplify the measurements. The double-sideband receiver sensitivity of the balanced mixer is 2-4 times the quantum noise limit  $h\nu/k_B$  over the measured frequencies with a maximum LO noise rejection of 15 dB. This work presents independent measurements with three different LO sources that produce the reference frequency but also an amount of near-carrier noise power which is quantified in the experiment as a function of the LO and IF frequency in terms of an equivalent noise temperature  $T_{LO}$ . Two types of LO sources are used: a synthesizer driven amplifier/multiplier chain and a Gunn oscillator driven multiplier chain. With the first type of LO we find different near-carrier noise contributions using two different power pre-amplifiers of the LO system. For one of the two power pre-amplifiers we measure  $T_{LO} = 30 \pm 4$  K at the LO frequency 380 GHz and  $T_{LO} = 38 \pm 10$  K at 420 GHz. At the frequency band center 465 GHz of the Gunn driven LO we measure a comparable value of  $T_{LO} = 32 \pm 6$  K. For the second power pre-amplifier a significant higher  $T_{LO}$  value of the synthesizer driven LO is found which is up to six times larger compared with the best values found for the Gunn driven LO. In a second experiment we use only one of two SIS mixers of the balanced mixer chip in order to verify the influence of near-carrier LO noise power on a single-ended heterodyne mixer measurement. We find an IF frequency dependence of near-carrier LO noise power. The frequency-resolved IF noise temperature slope is flat or slightly negative for the single-ended mixer. This is in contrast to the IF slope of the balanced mixer itself which is positive due to the expected IF roll-off of the mixer. This indicates a higher noise level closer to the LO's carrier frequency. Our findings imply that near-carrier LO noise has the largest impact on the sensitivity of a receiver system which uses mixers with a low IF band, for example superconducting hot-electron bolometer (HEB) mixers.

PACS numbers: 85.25.Pb, 07.57.-c, 84.30.Le

## I. INTRODUCTION

State-of-the-art low-noise heterodyne receivers are a key technology in radio astronomy and are needed to conduct high-resolution spectroscopy ( $\nu/\delta\nu \geq 10^6$ ) in the 0.3 - 5 terahertz (THz) frequency band. Here, among many fundamental astronomical objects, for example, star-forming regions have very rich atomic and molecular spectra<sup>1</sup>. The highest possible receiver sensitivity is needed because the signals which contain the astronomical information are usually very weak. For spectroscopy in the frequency band 0.3 - 1.2 THz, heterodyne receivers employ superconductor-insulator-superconductor (SIS) detectors as frequency mixing devices. They are operational up to frequencies of  $4\Delta/h$ , where  $\Delta$  is the superconducting gap energy of the detector electrodes. For frequencies larger than  $4\Delta/h$  where SIS devices do not work anymore, superconducting hot-electron bolometers (HEB) are used<sup>2</sup>. In a THz heterodyne receiver a weak

signal with frequency  $\nu_S$  is detected by multiplying it with a strong local oscillator (LO) reference signal with frequency  $\nu_{LO}$  in the SIS or HEB device where the intermediate frequency (IF)  $\nu_{IF} = |\nu_S - \nu_{LO}|$  is produced. Generally,  $\nu_{IF}$  ranges from 0 - 4 GHz for an HEB device or from 4 - 12 GHz for an SIS device. Heterodyne detection preserves amplitude and phase of the incoming signal. Therefore, Heisenberg's uncertainty principle imposes a fundamental limit<sup>3</sup> on the sensitivity usually expressed by a quantum noise temperature  $T_{qn} = h\nu_S/k_B$  for double-sideband operation,  $h$  and  $k_B$  are the Planck and Boltzmann constants.

For heterodyne receivers, presently two established LO technologies are used. Gunn oscillator driven multiplier chains<sup>4</sup> for frequencies up to approximately 0.8 THz and synthesizer driven amplifier/multiplier chains that are easier to operate and which are used for almost the whole THz frequency range, nowadays even exceeding 2 THz<sup>5,6</sup>. A Gunn driven LO consists of a III-V semiconductor (usually GaAs or InP) embedded in a mechanically tunable high-Q waveguide resonator which produces amplitude stable signals with high spectral purity and a very low amount of near-carrier noise power. A cascade of

<sup>a)</sup>westig@ph1.uni-koeln.de

Schottky diode frequency multipliers is used to produce the output frequency of the Gunn driven LO.

However, receivers in modern radio-astronomy experiments increasingly use synthesizer driven LO's due to their easy handling. First, the signal of the synthesizer is fed into a frequency multiplier, usually a doubler or a tripler. The output is connected to a power pre-amplifier which is connected to a cascade of frequency multipliers. With this technique frequencies up to approximately 2 THz can be produced. Mainly stimulated by receiver developments for ground-based and space observatories where strict performance specifications have to be fulfilled, it was found that synthesizer based LO sources have to be operated and designed following rules which are summarized in<sup>7-9</sup>. An important conclusion is that near-carrier LO noise power in these devices can be minimized if the input power saturates the LO components, i.e. the power pre-amplifier and the multiplier chain.

In the near future quantum cascade lasers (QCLs<sup>10</sup>) might offer another LO technology solving the problem of low output power for frequencies larger than 1 THz,<sup>11,12</sup> rendering the development of heterodyne cameras possible. Due to the laser operation a very low noise is expected for a QCL.

The most sensitive heterodyne receivers operate at a few times the quantum noise limit. Each element of the receiver, usually consisting of quasi-optics to focus the signal and the LO beam on the mixer, followed by a low-noise cryogenic IF amplifier,<sup>13-15</sup> additional low-noise amplifiers at room temperature and a spectrometer adds a noise contribution to the total receiver noise temperature  $T_{rec}$ . This can be analyzed by decomposition according to the *Friis* formula<sup>16</sup>. In practice,  $T_{rec}$  is measured with a standard *Y*-factor method<sup>17</sup>. LO near-carrier noise power which is among other things caused by a fluctuating LO amplitude (AM noise), is mixed down into the IF band, thus has a substantial impact on  $T_{rec}$  and results in a decrease of the receiver's sensitivity. However, in a heterodyne receiver with a single-ended mixer an unambiguous separation and quantification of the unknown amount of near-carrier LO noise power from other receiver noise contributions is not possible. Any noise from the LO sidebands is downconverted in the frequency mixing process and is at the end indistinguishable from the desired IF signal<sup>8</sup>. This shows that a single-ended mixer is very susceptible to this particular noise source.

Balanced mixers are much less sensitive to near-carrier LO noise power and offer the possibility of a direct quantification of the noise produced by the complete LO system. With this mixer technology it is possible to separate the LO AM noise from other noise sources of the heterodyne receiver. In the submm range this was not possible for a long time due to the complexity of building sensitive balanced mixers for these small wavelengths.

This paper is organized into four sections. Following the introduction, Sec. II describes the experimental setup and the noise measurement principle using a planar cir-

cuit balanced quasiparticle mixer device<sup>18</sup>. Section III presents the experiment. In the 380-520 GHz range we measure the near-carrier noise power produced by three different LO sources: a Gunn driven LO and a synthesizer driven LO with two different power pre-amplifiers. We show how to separate this unwanted noise contribution from the receiver system and quantify the equivalent near-carrier noise temperature  $T_{LO}$  by using our balanced mixer device as a noise meter. The impact of near-carrier noise power on single-ended mixers is studied in a second experiment and is used to verify our results. Here we observe that the IF spectra of the single-ended- and the balanced mixer measurements differ significantly. Sec. IV discusses the results and presents our conclusions. Especially the conclusion with regard to the spectral characteristic of the LO noise is relevant for THz HEB mixers that generally operate with a low IF band and where the balanced technology is not yet broadly established. In these mixers near-carrier noise power from the LO can substantially degrade the receiver's sensitivity.

## II. DESCRIPTION OF THE EXPERIMENT

### A. Experimental setup

Fig. 1 shows the experimental setup. The sketch of the LO shows the most important parts of this device, developed by Virginia Diodes Inc<sup>5</sup>. We use a synthesizer<sup>19</sup> with a measured phase noise of 115 dBc/Hz, 90 kHz away from the carrier frequency set to 11.806 GHz. We could not detect an amplitude noise contribution from the synthesizer in a time domain measurement with a spectrum analyzer<sup>20</sup>. The synthesizer is tuned either to a frequency between 10.7 - 12.2 GHz or to a frequency between 12.5 - 14.17 GHz and is connected to one of two actively biased frequency triplers. No frequency standard was used during our measurements. Each of the two triplers is connected to one of two power pre-amplifiers<sup>21</sup> PA1 and PA2. The power pre-amplifiers are biased with  $U_{bias} = 8 - 12$  V. A second bias voltage  $U_{sat} = 0 - 5$  V feeds an electronic attenuation circuit. For  $U_{sat} = 0$  V the maximum output power and for  $U_{sat} = 5$  V the maximum attenuation of PA1 and PA2 is chosen. A feedback loop (not shown in Fig. 1) measures the power delivered to the first module of the frequency multiplier chain, sets the output power correctly and protects it from an excess of input power. The frequency multiplier chain consists of three modules: two frequency doublers and a frequency tripler. For measurements using a Gunn driven LO, we replace the synthesizer driven LO. A rotatable polarization grid is used to attenuate the LO power independently from applying the voltage  $U_{sat}$ .

The mixer is only sensitive to the  $\vec{E}_{\perp}$  component of the LO's electric field which points perpendicularly out of the paper plane in Fig. 1. A 21  $\mu\text{m}$  thick Mylar foil is used as a beamsplitter to feed the LO signal into the dewar and provides the possibility to terminate window

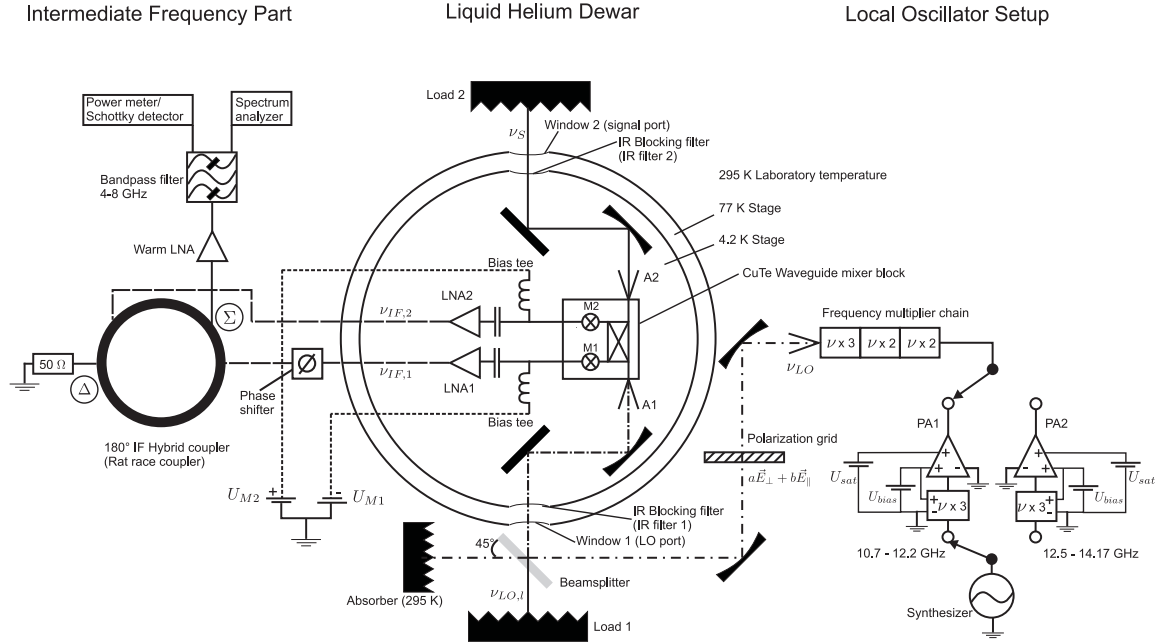


FIG. 1. Sketch of the experimental setup. The two SIS mixers (M1 and M2) of the balanced circuit are indicated with the  $\otimes$ -symbol and the crossed rectangle is the  $90^\circ$  hybrid coupler (compare also with Fig. 3). The combination of the separately amplified IF signals of the balanced mixer ( $\nu_{IF,1}$  and  $\nu_{IF,2}$ ) is done at room temperature (295 K) with a commercial  $180^\circ$  IF hybrid coupler. Two separate blackbody loads, load 1 (LO port) and load 2 (signal port), are used at a temperature of either 77 K or 295 K. Their noise power is used to measure  $T_{rec}$  and near-carrier LO noise power simultaneously. The measurement is performed with a bias voltage sweep of either  $U_{M1}$  or  $U_{M2}$  while the other mixer bias voltage is kept constant within the first photon-assisted tunneling step of the SIS IV characteristic. The combined IF power is read-out at the  $\Sigma$  output of the  $180^\circ$  IF hybrid coupler. In the synthesizer driven LO a switch is used to choose one of the two power pre-amplifiers (PA1 or PA2) for the measurement. In this experiment load 1 is used as a 77 K termination of the LO port in order to determine the LO noise and is removed in an astronomical receiver. Windows, IR blocking filters and beamsplitter each have a frequency dependent transmissivity which is determined in Sec. II B.

1 (LO port) with a thermal load of varying temperature (load 1 in Fig. 1). Window 1 consists of a  $426 \mu\text{m}$  thick slab of Teflon material. The IR blocking filter on the 77 K radiation shield behind window 1 is a slab of  $267 \mu\text{m}$  thick high-density polyethylene (HDPE). Window 2 (signal port) is made of a  $482 \mu\text{m}$  thick slab of Teflon and behind this window is a  $261 \mu\text{m}$  thick HDPE IR blocking filter, also on the 77 K radiation shield. The balanced mixer chip is assembled inside a gold plated tellurium copper split-block full-height waveguide mixer block. This mixer block is fixed in a cold optics assembly on the liquid helium (LHe) dewar 4.2 K cold stage. Load 1 in front of window 1 is used to terminate the LO port with a 77 K load throughout the experiment. Noise power from this load is superimposed with the LO signal. The thermal load in front of window 2 (load 2) is either cooled to 77 K or replaced by a 295 K load and serves as a calibration blackbody radiation source, representing the sky signal. LO signal and noise power from load 1 are transmitted through window 1 (LO port) while noise power from load 2 is transmitted through window 2 (signal port). Both signals are received by the balanced mixer via two waveguide horn antennas A1 and A2 (also

referred to as "mixer input ports" in the text). The signals are coupled into the balanced mixer chip where they are superimposed, phase shifted and equally distributed ( $-3 \text{ dB}$ ) to the two individual SIS mixers M1 and M2. Here the IF signals  $\nu_{IF,1}$  and  $\nu_{IF,2}$  are produced and are separately amplified by two MMIC WBA13 low noise amplifiers LNA1 and LNA2<sup>15</sup>. Outside of the LHe dewar the two IF signals are combined by a  $180^\circ$  IF hybrid coupler<sup>22</sup>. A phase shifter which is connected to the IF output port of M1 is used to adjust the phase between the IF frequency paths of M1 and M2 in order to achieve the best possible balanced performance. The combined IF signal is read-out at the  $\Sigma$  output (sum port) of the  $180^\circ$  IF hybrid coupler, and the  $\Delta$  output (difference port) is terminated by a  $50 \Omega$  load throughout the experiment. We use a power meter and a power calibrated Schottky detector, respectively, to measure the total IF output power over 4-8 GHz as a function of mixer bias voltage  $U_{M1}$  or  $U_{M2}$  while the other mixer is constant voltage biased within the first photon-assisted tunneling step of the SIS IV curve. Therefore, in a single bias voltage sweep of one of the two mixers, the balanced mixer provides two different measurement results. At the  $\Sigma$

TABLE I. Summary of the parameters used to determine the transmissivity and emissivity of the windows, IR blocking filters and the beamsplitter in the measurement bandwidth 380 - 520 GHz. The beamsplitter is rotated by  $45^\circ$  with respect to the LO beam axis.  $d$  is the thickness and  $n_d$  is the complex refractive index. The uncertainty (not shown in the table) of the values below is considered in the calculation of the uncertainty of the effective temperatures, summarized in Table II.

	$d$ [ $\mu\text{m}$ ]	$n_d$	Material
Window 1	426	$1.46 - i 0.0018$	Teflon
IR filter 1	267	$1.32 - i 0.0005$	HDPE
Beamsplitter	21	$1.80 - i 0.0320$	Mylar
Window 2	482	$1.52 - i 0.0020$	Teflon
IR filter 2	261	$1.22 - i 0.0005$	HDPE

output of the IF hybrid coupler for same bias polarity of mixers M1 and M2, LO noise power and the noise power coming from load 1 (LO port) is measured.  $T_{rec}$  is measured independently for opposite bias polarity of M1 and M2 at the same port of the IF hybrid coupler. For further details we refer to Sec. II C. A spectrum analyzer is used to measure the frequency resolved IF power signal with fixed mixer bias voltage where now both mixers are voltage biased within the first photon-assisted tunneling step.

## B. Effective load temperature

To determine the effective load temperatures (Rayleigh-Jeans limit) at the mixer input ports A1 and A2, respectively, the transmissivity and emissivity of the IR blocking filters and the vacuum windows in front of both input ports and of the beamsplitter in front of A1 have to be known. The IR blocking filters have a temperature of approximately 85 K, measured in an earlier experiment with a temperature sensor. Window 1, window 2 and the beamsplitter have a temperature of 295 K. Transmissivity is measured using a Fourier transform spectrometer (FTS) working in the frequency range 1 - 6 THz from which we obtain the frequency dependent gain  $G(\nu) < 1$  of each element. Moreover, in our high-frequency measurement bandwidth the individual complex refractive index  $n_d = n'_d - in''_d$  of the IR blocking filters, windows and the beamsplitter is not known. Furthermore, polishing of the dielectric materials to the nominal size is expected to further modify the dielectric properties. Fourier transform spectrometry provides a straightforward determination method of the individual characteristics of each element. Finally, the *Fresnel* theory is used to fit the experimental data and to extrapolate the transmissivity to our measurement bandwidth 380 - 520 GHz where the FTS detector is not sensitive enough for a direct measurement. For the beamsplitter the transmissivity is evaluated for an angle

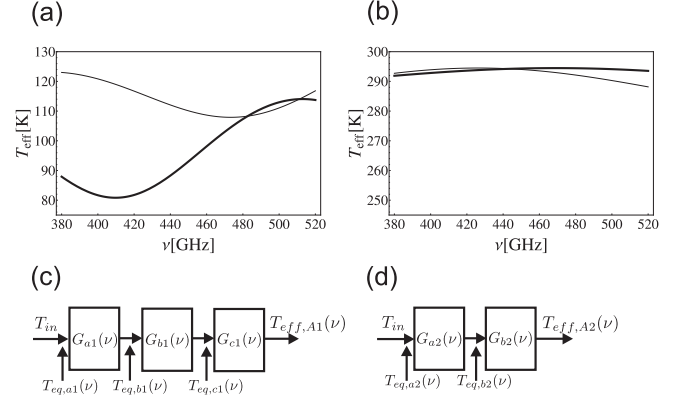


FIG. 2. In (a) for  $T_{in} = 77$  K and in (b) for  $T_{in} = 295$  K the effective load temperatures are calculated for frequencies in the measurement bandwidth. The thin solid lines in (a) and (b) show the effective load temperature  $T_{eff,A1}$  referred to mixer input port A1 and the thick solid lines show  $T_{eff,A2}$  referred to mixer input port A2. Equivalent circuit diagrams for the window-IR filter-beamsplitter and window-IR filter cascade in front of mixer input ports A1 and A2 are shown in (c) and (d).

of  $45^\circ$  relative to the LO beam axis. Free parameters of the fit are the thickness  $d$  and the complex refractive index of the slab, the results are summarized in Table I. The results of the fits are used further to calculate the effective load temperatures as a function of frequency.

A thermal load having a temperature  $T_{in}$  of either 77 K or 295 K in front of window 1 yields at the mixer input port A1 an effective temperature of

$$T_{eff,A1}(\nu) = G_{a1}(\nu)G_{b1}(\nu)G_{c1}(\nu)(T_{in} + T_{eq,a1}(\nu)) + G_{b1}(\nu)G_{c1}(\nu)T_{eq,b1}(\nu) + G_{c1}(\nu)T_{eq,c1}(\nu). \quad (1)$$

The indices  $a1, b1$  and  $c1$  relate the respective gains and equivalent noise temperatures to the beamsplitter, to window 1 and the IR filter 1. For each element, the emissivity is written in terms of an equivalent input noise temperature which is given by the formula

$$T_{eq}(\nu) = T_{phys} \frac{1 - G(\nu)}{G(\nu)}, \quad (2)$$

with  $T_{phys}$  being the physical (ambient) temperature of the element. Similarly, the effective load temperature  $T_{eff,A2}(\nu)$  is calculated where only the dewar window and the IR filter contribute. Figures 2(a) and 2(b) show the results for the effective temperatures. Figures 2(c) and 2(d) present equivalent circuits for the window-IR filter-beamsplitter and window-IR filter cascade in front of mixer input port A1 (LO port) and A2 (signal port).

### C. LO noise measurement using a balanced mixer

A LO signal with sideband noise is written in terms of a time-varying voltage

$$V_{LO}(t) = \tilde{V}_{LO}e^{i\omega_{LO}t} + V_n(t), \quad (3)$$

where  $\tilde{V}_{LO}$  is the LO amplitude and  $\nu_{LO} = \omega_{LO}/2\pi$  is the LO fundamental frequency. In Eq. (3) the second term describes the near-carrier AM noise contribution to the LO signal

$$V_n(t) = \sum_{k=-\infty}^{\infty} c_k e^{i\omega_k t}. \quad (4)$$

Generally, it has many frequency components  $\omega_k$  near the carrier  $\omega_{LO}$  and the expansion coefficients  $c_k$  can in principle be determined by Fourier analyzing the signal. In our experiment a blackbody signal with frequencies  $\nu_S$  is applied to A2 (signal port) and the LO signal together with noise (Eq. 3) is applied to A1 (LO port) of the probably not ideal balanced mixer shown in Fig. 3. A not ideal balanced mixer has two mixers M1 and M2 with different gains  $G_{M1} \neq G_{M2}$ , the  $90^\circ$  hybrid coupler is not symmetric with respect to the two output ports connecting the two mixers,  $\tau^2 \neq \rho^2$ , and a phase error between the two output ports of the  $90^\circ$  hybrid coupler occurs, i.e.  $\delta\varphi \neq 0^\circ$ . This modifies the  $Y$ -factor of the receiver with respect to input A2 of the mixer which generally reads

$$Y = \frac{T_{eff,A2,h} + T_{eff,A1,c} \cdot \frac{1}{NR} + \tilde{T}_{rec}}{T_{eff,A2,c} + T_{eff,A1,c} \cdot \frac{1}{NR} + \tilde{T}_{rec}} \quad (5)$$

for a non-ideal device, where  $NR$  is the noise rejection ratio defined by Eq. (6). Equation (5) is obtained by applying the standard balanced mixer theory to our device in which  $NR$  contains all imperfections of the mixer.

At the  $\Sigma$  output of a  $180^\circ$  IF hybrid coupler shown in Fig. 1, the combined (sum) current from the SIS mixers M1 and M2 can be measured. At the  $\Delta$  output of the same IF hybrid coupler the IF current of M2 is shifted by an additional phase of  $-\pi$  with respect to the IF current of M1 and the resulting IF (difference) current can be measured. Reversing the bias polarity for M1 or M2, the output ports of the  $180^\circ$  IF hybrid coupler are exchanged, i.e.  $\Delta \leftrightarrow \Sigma$ . For example, reading out the signals at the  $\Sigma$  output of the IF hybrid coupler and sweeping the bias voltage of M1 from negative to positive values while M2 is kept constant at a negative voltage, shows the noise power from the LO port in the negative half of the voltage sweep and the signal power in the positive half without having to swap the power meter between the two IF hybrid output ports.

A more detailed discussion of the balanced mixer theory can be found in<sup>23-25</sup>. The fundamental calculation of the IF current of a SIS mixer or its gain is provided

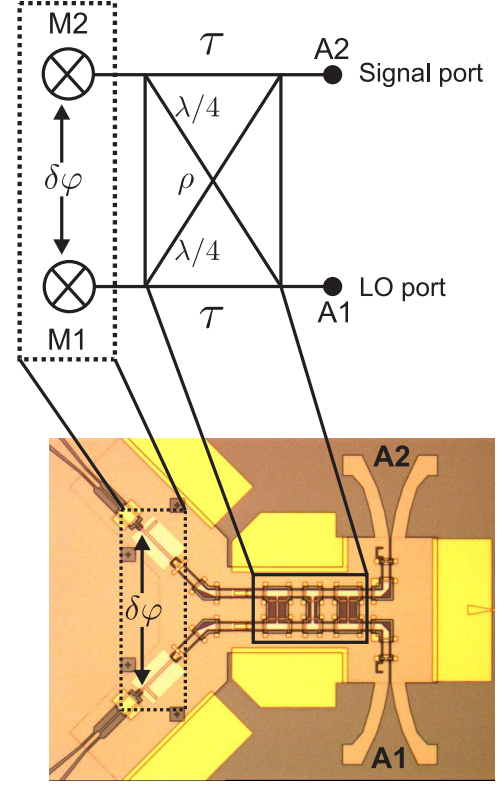


FIG. 3. Top: Balanced mixer circuit diagram showing the two mixer input ports A1 and A2, the  $90^\circ$  hybrid coupler (crossed rectangle) and the two SIS mixers M1 and M2 having gains  $G_{M1}$  and  $G_{M2}$ .  $\tau^2$  and  $\rho^2$  are power coupling factors and  $\delta\varphi$  is the phase error of a possibly not ideal  $90^\circ$  hybrid coupler. Bottom: Detail photograph of the mixer chip focussing on the RF part of the circuit.

by Tucker and Feldman in the framework of the quantum theory of mixing<sup>26</sup> and is outside of the scope of this paper.

In summary, in this paper the negative half of the voltage sweep represents the window 1 (LO noise) port and the positive half represents the window 2 (signal) port. This provides the possibility to determine  $T_{rec}$  and near-carrier LO noise in one voltage sweep of mixer M1 or M2 from e.g. -4 mV to +4 mV while the other mixer bias voltage is kept constant within the first photon-assisted tunneling step (Fig. 8(b)). The combined signal is read-out at the  $\Sigma$  output of the IF hybrid coupler, see Figs. 4 and 5.

For a better understanding of our measurement results, a qualitative comparison of an ideal gain performance of the mixers and the  $90^\circ$  hybrid coupler with a non-ideal device is discussed below by using Fig. 4. For simplicity, we assume for the moment that windows 1 and 2, both IR blocking filters and the beamsplitter have a transmissivity of 1, i.e. the temperature of load 1 and 2 is not modified by the dielectrics. Furthermore, for our qual-

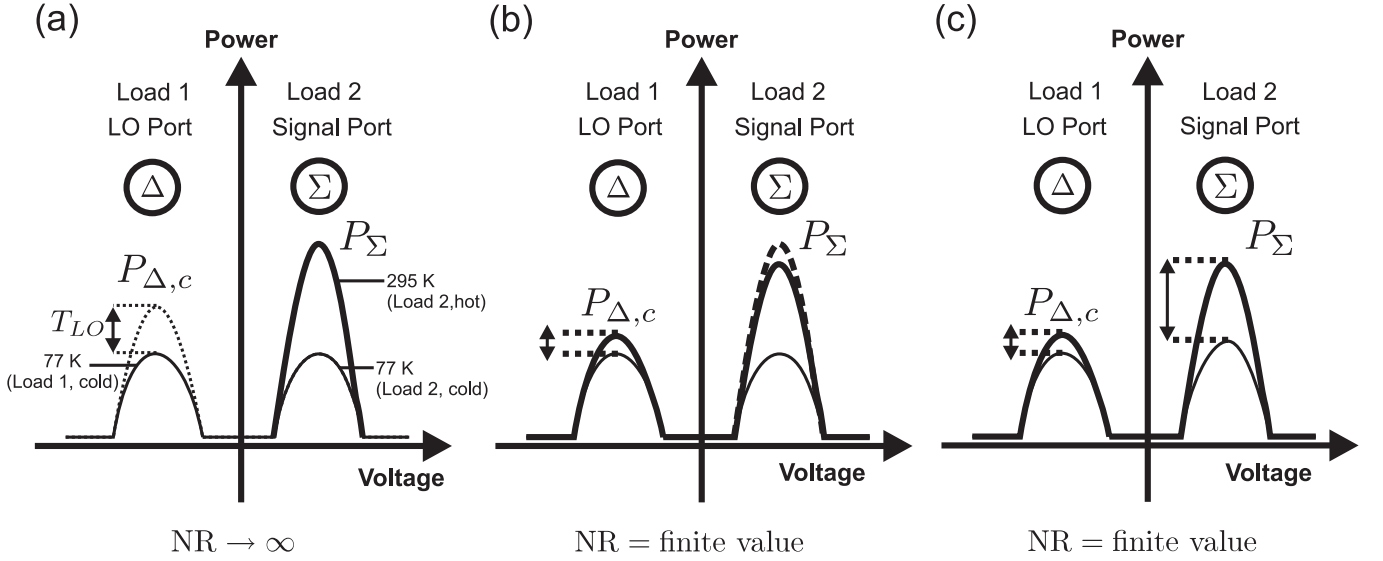


FIG. 4. Schematic representation of the balanced SIS mixer IF output power trace for three cases (a)-(c). One of the two SIS mixers on the balanced mixer chip is constantly biased with a negative voltage within the first photon-assisted tunneling step. A voltage sweep is applied to the other mixer. Power coming from load 1 (LO port) is measured in the  $\Delta$  output ( $P_{\Delta,c}$ ) whereas power coming from load 2 (signal port) is measured in the  $\Sigma$  output ( $P_{\Sigma}$ ) of the IF output power trace. Thick solid lines show measurements where load 2 has a temperature of 295 K whereas thin solid lines show measurements with a load temperature of 77 K. Load 1 has a constant temperature of 77 K. For each case it is indicated whether the noise rejection value ( $NR$ , Eq. (6)) is infinite or takes a finite value. (a) Ideal balanced mixer. Temperatures are equivalent values through the relation  $P = Tk_B B G_{rec}$ , where  $G_{rec}$  is the receiver gain,  $T$  is the input temperature of either 295 or 77 K and  $B$  is the IF bandwidth. The effect of near-carrier LO noise with equivalent noise temperature  $T_{LO}$  is to increase the power  $P_{\Delta,c}$  above the corresponding input noise power  $77 \cdot k_B B$  from load 1. (b) shows the effect of unequal mixer gain on the balanced mixer's IF output power for  $\rho^2 = \tau^2 = 1/2$  and  $\delta\varphi = 0^\circ$  or the effect of an asymmetry in the  $90^\circ$  hybrid coupler for equal mixer gain and  $\delta\varphi = 0^\circ$ . The dashed line indicates the ideal case for the  $\Sigma$  output in which the distance between the dotted lines in the  $\Delta$  output approaches zero. (c) Most likely situation during the experiment. In order to achieve the best balanced mixer performance, the difference between the two traces in the  $\Delta$  output has to be minimized while maximizing the difference of the two traces in the  $\Sigma$  output (arrows) which is achieved by adjusting the phase shifter in the IF path (Fig. 1).

itative explanation in this section we assume at first a noiseless LO and then describe how the balanced mixer response changes when the LO has near-carrier noise.

**Case 1:**  $G_{M1} = G_{M2}$ ,  $\rho^2 = \tau^2 = 1/2$  and  $\delta\varphi = 0^\circ$ .

This is the ideal case and is qualitatively shown in Fig. 4(a). If the LO would have near-carrier noise of equivalent temperature  $T_{LO}$ , a larger noise power than just the noise power from a 77 K load is measured. The same effect would occur for the following cases 2-3. In order to better understand the non-ideal balanced mixer response, for clarity these cases are discussed assuming no LO noise.

**Case 2:**  $G_{M1} \neq G_{M2}$ ,  $\rho^2 = \tau^2 = 1/2$  and  $\delta\varphi = 0^\circ$  or  $G_{M1} = G_{M2}$ ,  $\rho^2 \neq \tau^2 = 1/2$  and  $\delta\varphi = 0^\circ$ .

This case is illustrated in Fig. 4(b) for a 295 K load (thick solid line) in front of window 2 (signal port) and for a 77 K load in front of window 1 (LO port). The measured noise power  $P_{\Delta,c}$  is in excess of  $77 \cdot k_B B$  (arrow) and the height of  $P_{\Sigma}$  for a 295 K load is lower than in the ideal case (dashed line). When translating near-carrier LO noise power into an equivalent noise temperature,

the difference between the measured noise power in the  $\Delta$  output when load 2 (signal port) is varied between 77 K and 295 K is a major uncertainty of the measurement.

**Case 3:**  $G_{M1} \neq G_{M2}$ ,  $\rho^2 \neq \tau^2$  and  $\delta\varphi \neq 0^\circ$ .

This is the most realistic case observed in the experiment and is shown in Fig. 4(c). Both the negative and the positive half of the IF output power trace are influenced from the measured noise power. During the experiment the minimum of  $T_{rec}$  measured at the  $\Sigma$  output and the minimum of residual noise power from load 2 measured at the  $\Delta$  output, is adjusted with the phase shifter, therefore, finding the maximal value for  $NR$ .

### III. LO NOISE MEASUREMENTS

#### A. Quantitative LO noise determination

This section presents heterodyne measurements using the balanced SIS mixer with three different LO sources: a Gunn LO and a synthesizer LO which uses two different

power pre-amplifiers (PA1 and PA2 in Fig. 1). We use the mixer as a noise meter and quantify residual near-carrier LO noise power produced by the LO. The synthesizer LOs are optimally operated, i.e. with input power saturating all of its components. For the measurements the output power of PA1 or PA2 was set to its maximum value and the synthesizer output power was 16 dBm. Adjustment of the optimal coupled power of the synthesizer LO to the mixer was achieved using a polarization grid (Fig. 1). The Gunn driven LO was used for comparison measurements as we expect that this device produces less near-carrier LO noise than the synthesizer driven LO.

We start by describing our method of measuring near-carrier LO noise and how this method is implemented in our experiment. One of the two mixers M1 or M2 is kept at a constant bias voltage within the first photon-assisted tunneling step of the SIS IV curve. The total IF output power is measured at the  $\Sigma$  output of the  $180^\circ$  IF hybrid coupler for opposite bias polarity of M1 and M2 and for two different temperatures  $T_{L2}$  (295 K and 77 K) of load 2 while the  $\Delta$  output is terminated with a  $50 \Omega$  load. During all measurements load 1 is kept at a constant temperature of  $T_{L1} = 77$  K. For opposite bias polarity of M1 and M2, we denote the total IF output power by  $P_\Sigma$ , measured at the  $\Sigma$  output. This signal is the one shown in the positive half of the power traces in Fig. 5. An analogous measurement is performed with same bias polarity of the two mixers where we measure  $P_\Delta$  at the  $\Sigma$  output. This signal is the one shown in the negative half of the power traces.

Figure 5 shows typical results of the measured balanced mixer total IF output power using the synthesizer LO [(a) and (b)] and the Gunn LO [(c) and (d)]. We measure the noise power emitted from load 2 received by mixer input port A2 (signal port) and the superposition of noise power emitted from load 1 with near-carrier LO noise power which is received by mixer input port A1 (LO port). The combined signals are read-out at the  $\Sigma$  output of the  $180^\circ$  IF hybrid coupler shown in Fig. 1.

An ideal balanced mixer separately measures  $P_\Sigma$  and  $P_\Delta$  and provides the possibility to quantify any noise signal received by mixer input port A1 (LO port), contained in  $P_\Delta$  and shown in the negative part of the IF output power trace, independent of the signal  $P_\Sigma$  received by A2 (signal port) and which is shown in the positive part of the IF output power trace. The isolation between the two distinct signals  $P_\Sigma$  and  $P_\Delta$  determines the quality of the balanced mixer. A criterion for the isolation is the noise rejection value  $NR$  defined as

$$NR = \frac{dP_\Sigma}{dP_\Delta} . \quad (6)$$

In the equation,  $dP_\Sigma$  is the IF output power difference for opposite mixer bias polarity when load 2 has a temperature of 295 K and 77 K and  $dP_\Delta$  is the IF output power difference for same bias polarity.

For the rest of the paper we assume that  $NR$  is sufficiently large so that Eq. (5) takes the form of Eq. (8).

The values for  $NR$  which we determine from our measurements, summarized in Table II, justifies this simplification. For the lowest  $NR$  values, the introduced uncertainty to the measured value of  $\tilde{T}_{rec}$  is approximately one standard deviation and for higher  $NR$  values, accordingly, it is less.

For the data analysis, in the negative and positive half of the IF output power trace the noise power from the two loads and the near-carrier LO noise power can be quantified (compare with Fig. 4). The Gunn LO is tuned to frequencies of 445, 465 and 495 GHz. Measurements at frequencies 380, 420, 460 and 490 GHz use the synthesizer LO.

The IF output power values  $P_\Sigma$  for the individual LO frequencies obtained for the temperatures  $T_{L2}$  of load 2 have to be related to the respective effective temperatures as seen by the two mixer input ports A1 and A2. For this purpose, a  $Y$ -factor measurement determines  $T_{rec}$ . Furthermore, the  $Y$ -factor relates  $P_\Sigma$ ,  $T_{L2}$  and  $T_{rec}$

$$Y = \frac{T_{L2,h} + T_{rec}}{T_{L2,c} + T_{rec}} = \frac{P_{\Sigma,h}}{P_{\Sigma,c}} , \quad (7)$$

where  $P_{\Sigma,h}$  and  $P_{\Sigma,c}$  are the receiver IF output powers measured when load 2 (signal port) has a temperature of  $T_{L2,h} = 295$  K and  $T_{L2,c} = 77$  K. Equation (7) yields the same result, but is more suitable for our experiment when correcting  $T_{L2}$  and  $T_{rec}$  for the thermal noise contribution coming from the dielectric slabs in front of mixer input port A2

$$Y = \frac{T_{eff,A2,h} + \tilde{T}_{rec}}{T_{eff,A2,c} + \tilde{T}_{rec}} = \frac{P_{\Sigma,h}}{P_{\Sigma,c}} . \quad (8)$$

In the equation above,  $T_{eff,A2,h}$  is the effective temperature seen by mixer input port A2 when load 2 (signal port) has a temperature of 295 K ("hot load", h) while  $T_{eff,A2,c}$  is the effective temperature for a load temperature of 77 K ("cold load", c).  $\tilde{T}_{rec}$  is the corrected receiver noise temperature with respect to the effective temperature. Table II summarizes the measured values for  $\tilde{T}_{rec}$  showing the close to quantum limited performance of our receiver which is in the range of 2-4  $h\nu_S/k_B$ . In the same table, the column summarizing the effective temperatures  $T_{eff,A1,c}$  seen by mixer input port A1 (LO port) contains two numbers. The first number outside of the brackets is the effective temperature calculated in Sec. II B for the temperature 77 K of load 1 and is used for comparison. The second number inside of the brackets is the effective temperature plus the equivalent noise temperature of the LO obtained from a calculation using the equation

$$P_{\Delta,c} = \frac{T_{eff,A1,c} + T_{LO} + \tilde{T}_{rec}}{T_{eff,A2,h} + \tilde{T}_{rec}} P_{\Sigma,h} \quad (9)$$

In the following we explain in detail the idea behind this equation and its derivation. The starting point is Eq. (8). A perfect balanced mixer is symmetric with

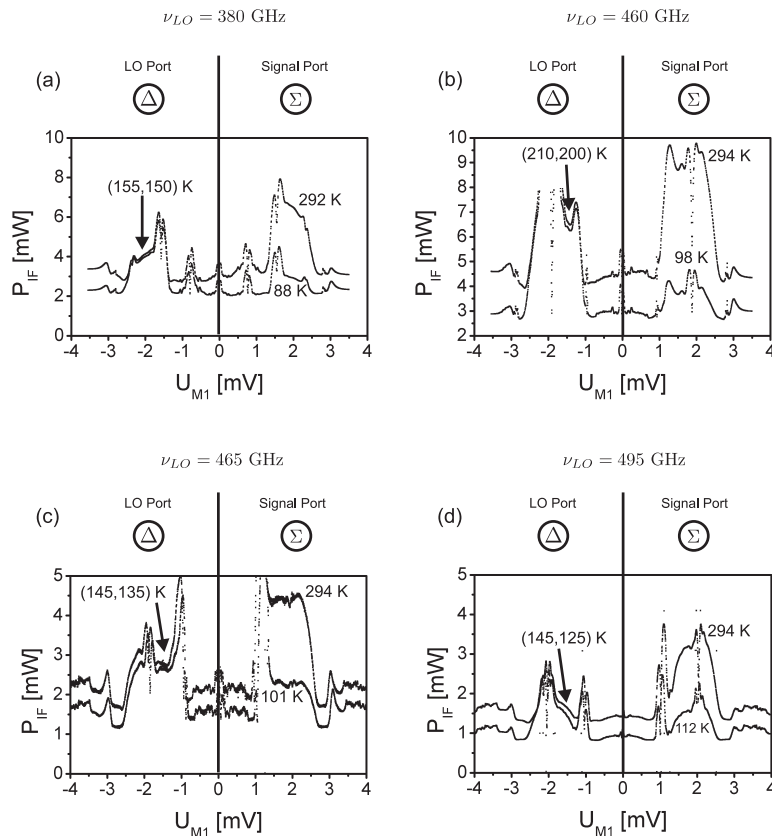


FIG. 5. Total IF output power of the balanced SIS mixer as a function of  $U_{M1}$  measured over the IF frequency range 4–8 GHz with a power meter. Mixer M2 is constantly biased at a negative voltage within the first photon-assisted tunneling step resulting in a relative shift between a pair of measurements for voltages larger or smaller than the photon-assisted tunneling step of M1 (for example from -1 mV to 1 mV). This detail is omitted in Fig. 4. Temperature values in the  $\Sigma$  output of the figure indicate the effective temperature of load 2 as seen from mixer input port A2 (signal port). The  $\Delta$  output measures the total temperature as seen from mixer input port A1 (LO port), i.e. the effective temperature of load 1 together with a possible temperature contribution from the LO caused by near-carrier noise power. Arrows point to the bias region in which the temperature is measured. The traces in (a) and (b) were measured using the synthesizer driven LO whereas the traces in (c) and (d) were measured using the Gunn driven LO.

respect to its two output ports and assuming for the moment that no additional external noise source (such as the noise power coming from the LO in our experiment) is present this allows to conduct a  $Y$ -factor measurement with either load 1 (LO port) or load 2 (signal port) with the same measurement result. To measure the IF output power, the mixers M1 and M2 would have same bias polarity when load 1 is used as a calibration blackbody source and opposite bias polarity when load 2 is used. It would even be possible to use the two loads together, say with load 1 having a temperature of 77 K and load 2 having a temperature of 295 K, again using the  $\Sigma$  output of the IF hybrid coupler. Using Eq. (8), with  $P_{\Sigma,h}$  being the measured noise power from load 2 and  $P_{\Sigma,c} = P_{\Delta,c}$  being the measured noise power from load 1, would give the same  $Y$ -factor as before using only one load for the measurement. If an unknown amount of noise power is superimposed with the noise power coming from one of the two loads, the  $Y$ -factor changes and gives us the op-

portunity to measure the noise power. In our experiment the noise power coming from load 1 (LO port) having a temperature of 77 K is increased by the near-carrier LO noise power (Fig. 4(a)). We measure first the  $Y$ -factor,  $Y = P_{\Sigma,h}/P_{\Sigma,c}$ , which we obtain from a measurement using load 2 (signal port), having two different temperatures of  $T_{L2,h} = 295$  K and  $T_{L2,c} = 77$  K. From this measurement,  $\bar{T}_{rec}$  is calculated using Eq. (8) and is summarized in Table II. The indicated uncertainty is the root-mean-square deviation which we obtained from a series of identical measurements. In an ideal balanced mixer, noise power received by mixer input port A1 (LO port) can be independently measured from the noise power received by mixer input port A2 (signal port), therefore, we substitute  $P_{\Sigma,c} \rightarrow P_{\Delta,c}$ . In order to fulfill Eq. (8), we substitute  $T_{eff,A2,c} \rightarrow T_{eff,A1,c} + T_{LO}$ . Solving for  $P_{\Delta,c}$  results in Eq. (9).  $T_{LO}$  is used as a free parameter in order to fit the right-hand side of this equation to the measured value of  $P_{\Delta,c}$ . The two numbers enclosed by the brackets

TABLE II. Summary of the LO noise measurements using a balanced SIS mixer. The column summarizing the values for  $T_{eff,A1,c}$  includes a second number in brackets which is the value  $T_{eff,A1,c} + T_{LO}$ . The equivalent LO noise temperature,  $T_{LO}$ , is listed in a separate column. At 465 GHz, the Gunn driven LO has very little output power resulting in an unusual large  $\tilde{T}_{rec}$  value compared to the result using a similar frequency for the synthesizer driven LO.

$T_{L1}$ [K]	$T_{L2}$ [K]	$\nu_{LO}$ [GHz]	$T_{eff,A1,c}$ [K]	$T_{eff,A2}$ [K]	$\tilde{T}_{rec}$ [K]	$T_{LO}$ [K]	NR [dB]
Gunn LO							
77	295	445	$122 (145) \pm 2$	$294 \pm 2$	$90 \pm 5$	$15 \pm 10$	$12 \pm 1$
	77		$122 (128)$	91			
77	295	465	108 (145)	294	100	$32 \pm 6$	14
	77		108 (135)	101			
77	295	495	110 (145)	294	50	$15 \pm 10$	10
	77		110 (125)	112			
Synthesizer LO							
77	295	380	123 (155)	292	80	$30 \pm 4$	15
	77		123 (150)	88			
77	295	420	117 (165)	294	90	$38 \pm 10$	10
	77		117 (145)	82			
77	295	460	109 (210)	294	40	$96 \pm 6$	15
	77		109 (200)	98			
77	295	490	109 (170)	294	60	$56 \pm 6$	12
	77		109 (160)	111			

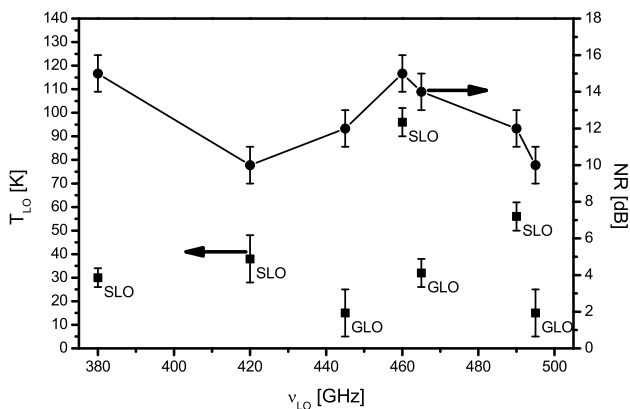


FIG. 6. Equivalent noise temperature  $T_{LO}$  (■) and noise rejection  $NR$  (●) as a function of LO frequency  $\nu_{LO}$ . Datapoints labeled with the abbreviation SLO were measured using the synthesizer LO whereas datapoints labeled with GLO belong to measurements which used the Gunn LO.

in Table II are the values  $T_{eff,A1,c} + T_{LO}$ , obtained for load 2 temperatures  $T_{L2,h} = 77$  K and  $T_{L2,h} = 295$  K. The mean value of the two measurements is summarized in the  $T_{LO}$  column for each LO frequency investigated in our experiment. A conservative estimate for the uncertainty in  $P_{\Sigma}$  and  $P_{\Delta}$  is 0.1 mW (1% - 3%) due to the power variation within the bias region where the noise power is measured. The uncertainty in  $T_{eff,A1,c}$  and  $T_{eff,A2}$  is determined from the fit to the measured transmissivity using the FTS described in Sec. IIB and the

result is 2 K. The uncertainty of  $T_{LO}$  is thus determined by the uncertainty of the fit to the FTS transmissivity data and by the difference between the mean value of  $T_{eff,A1,c} + T_{LO}$  and the single measurements when load 2 has temperatures of either  $T_{L2} = 295$  K or 77 K. This difference is a result of non-ideal balanced mixer performance. The noise rejection  $NR$  is corrected for the transmissivity of the dielectric slabs in front of mixer input port A2 and its uncertainty is mainly dominated by the uncertainties of  $P_{\Sigma}$  and  $P_{\Delta}$ . All results are summarized in Table II and in Fig. 6.

Measurements with the synthesizer driven LO for the two frequencies 380 GHz and 420 GHz used the power pre-amplifier PA1 and for the two higher frequencies 460 GHz and 490 GHz the power pre-amplifier PA2. Evidently, within the tolerance of our measurement, using PA2 an up to three times larger LO noise contribution could be measured compared to measurements using PA1. A measurement using the Gunn driven LO at 465 GHz resulted in the highest value of  $T_{LO}$  for this LO device, however, which was comparable with the synthesizer driven LO measurements at 380 GHz and 420 GHz. Gunn driven LO measurements at 445 GHz and 495 GHz resulted in the lowest values for  $T_{LO}$ . These values are a factor of 2 smaller than the LO noise values obtained with the synthesizer driven LO using PA1 and a factor of 4 - 6 smaller than the values obtained with the synthesizer driven LO using PA2.

## B. Effect of LO noise on single ended mixer performance

This section investigates the impact of LO noise power on a single-ended mixer which does not provide noise rejection like a balanced mixer. The results are used to verify our results from the previous section. In particular, our findings are interesting for a better understanding of the noise performance of single-ended mixers working in a frequency range where no or only few balanced mixer technologies are available.

Figure 7 shows a circuit diagram illustrating our measurement method employed to determine the influence of LO noise power on the single-ended mixer performance. The balanced mixer circuit, used in the previous section, is operated with one of two mixers voltage biased far above the superconducting gap voltage, therefore, being in the normal conducting state. This mixer is used as an absorber, terminating one branch of the  $90^\circ$  hybrid coupler. It is important to mention that in our device, noise generated by a mixer in the normal conducting state does not influence the heterodyne measurement using the other mixer by adding e.g. additional noise. Following the quantum tunneling theory, quasiparticles driven by a constant voltage  $V$  through an SIS junction generate current noise which can be written as<sup>27</sup>

$$\langle i^2(\nu) \rangle = e \left[ I \left( V + \frac{h\nu}{e} \right) \coth \left( \frac{eV + h\nu}{2k_B T} \right) + I \left( V - \frac{h\nu}{e} \right) \coth \left( \frac{eV - h\nu}{2k_B T} \right) \right], \quad (10)$$

illustrating a fluctuation-dissipation relation which connects the spectral quasiparticle current noise per unit bandwidth to the quasiparticle current response  $I(\dots)$ . For large voltages  $eV \gg k_B T$  and low frequencies for which  $eV \gg h\nu$ , the current noise is  $\langle i^2(\nu) \rangle \approx 2eI(V) \coth(eV/2k_B T)$  which is the usual shot noise formula, to good approximation independent of  $\nu$ . Intermediate frequency shot noise is not transmitted by the MIM capacitors separating the two SIS junction circuits in the balanced mixer<sup>18</sup> until  $\nu = 30$  GHz. For high frequencies the current noise approaches thermal equilibrium

$$\langle i^2(\nu) \rangle \approx e \left[ I \left( \frac{h\nu}{e} \right) - I \left( -\frac{h\nu}{e} \right) \right] \coth \left( \frac{h\nu}{2k_B T} \right). \quad (11)$$

In this limit the noise arriving at the other SIS junction circuit on the balanced mixer chip is determined by the isolation of the two branches of the  $90^\circ$  hybrid coupler. In the detection bandwidth 380-520 GHz, we derive by electromagnetic field simulation of the mixer chip an isolation value between the two mixers of -18 dB to -25 dB. This suggests that the contribution described by Eq. (11) can be neglected as well.

The other mixer is operated at voltages within the first photon-assisted tunneling step and is used as a heterodyne mixer. An ideal  $90^\circ$  hybrid coupler distributes one half of each signal received by mixer input ports A1 and

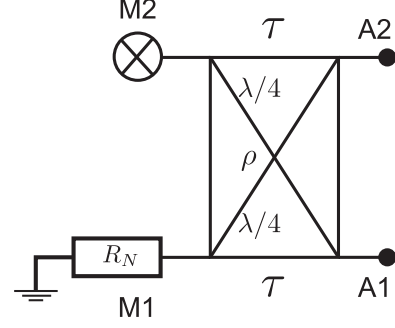


FIG. 7. Circuit diagram showing the measurement principle used to study the impact of LO noise power on a single-ended mixer. For an ideal  $90^\circ$  hybrid coupler, half of the signals received by the mixer input ports A1 and A2 are detected by M2 whereas half of the signals are absorbed by mixer M1. This is the case for  $\tau^2 = \rho^2 = 1/2$ . M1 is operated in the normal conducting state with resistance  $R_N \approx 21 \Omega$ . Because of symmetry, the same principle applies to M2 being operated in the normal conducting state where now M1 is used as mixer.

A2 to the two mixers. As can be seen in Fig. 8(b), to a good approximation this is the case for the frequency  $\nu_{LO} = 460$  GHz. The measurement of the single-ended mixer receiver noise temperature for  $\nu_{LO} = 460$  GHz with the synthesizer driven LO results in  $T'_{rec} = 100$  K for M1 and  $T'_{rec} = 78$  K for M2. A standard Y-factor method was conducted where first the combination of the noise power of load 1 and 2 both at a temperature of 77 K are measured using mixer M1 and M2 and subsequently the same measurement is performed for both loads at a temperature of 295 K.  $T'_{rec}$  is the receiver noise temperature without taking into account the noise power contribution of the LO but after correcting for the noise contribution of the dielectric slabs in front of the mixer input ports A1 and A2. In contrast to the result of  $\tilde{T}_{rec} = 40$  K obtained from our balanced measurement at  $\nu_{LO} = 460$  GHz, by using only the single-ended mixer obviously a larger receiver noise temperature is measured. In the previous section, we found an LO noise contribution of  $T_{LO} = 96$  K at 460 GHz. This means, by assuming an ideal coupler, the LO noise contributes 96/2 K noise to each of the two mixers in addition to the contribution of load 1 (LO port). Considering the effective temperatures  $T_{eff,A1}$  and  $T_{eff,A2}$  for a load temperature of 295 K and taking into account the additional LO noise power contribution superimposed with the noise power emitted by load 1, results in a total effective temperature of 342 K referred to the input of M1 and M2. Similarly when load 1 and 2 have a temperature of 77 K this results in a total effective temperature of 152 K with respect to the input of both mixers. Recalculating the single-ended mixer receiver noise temperature with these input temperatures results in  $\tilde{T}_{rec} = 50$  K for M1 and  $\tilde{T}_{rec} = 30$  K for M2 re-

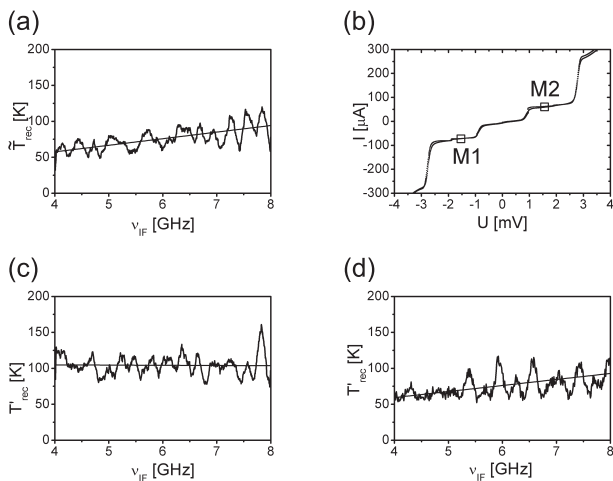


FIG. 8. (a)  $\tilde{T}_{rec}$  of the balanced mixer for  $\nu_{LO} = 460$  GHz using a synthesizer LO. (b) Rectangles show the bias voltages of the two mixers M1 and M2 during the measurement of the trace shown in (a). The figure shows two LO pumped SIS IV curves which are almost equal demonstrating the optimal device performance for this frequency. In (c) a single-ended measurement with mixer M2 at  $\nu_{LO} = 460$  GHz is presented which uses the synthesizer LO and during which  $U_{M1} = -5$  mV. The receiver noise temperature is corrected for the effective load temperatures with respect to both mixer input ports A1 and A2. (d) shows the result of a single-ended measurement using mixer M2 where again  $U_{M1} = -5$  mV and for  $\nu_{LO} = 455$  GHz. Instead of using the synthesizer driven LO we employed a Gunn driven LO for the measurement which results in a similar performance like observed in (a).

producing the balanced receiver noise temperature within a range of 10 K and justifying our result for  $T_{LO}$ . The balanced receiver noise temperature is not altered by LO noise to good approximation, provided that the quality of the balanced mixer operation is sufficiently good, as in our experiment. Throughout all frequencies within the operation bandwidth of the mixer, we observe that the performance of M1 is slightly inferior to that of M2 and we find that the balanced performance is about the average of both. The expected effect of LO noise power on the performance of a single-ended mixer receiver is to add  $T_{LO}$  to  $T_{rec}$ . Using an LO with a significant noise power contribution and comparing  $T_{rec}$  as a function of  $\nu_{IF}$  for a balanced and a single-ended mixer an interesting difference between both IF traces is observed. In Fig. 8 we show such a measurement in (a) for the balanced mixer and in (c) for a single-ended measurement using mixer M1. Both measurements were conducted with the synthesizer driven LO. From a linear fit to the two IF traces we find for the balanced mixer measurement a positive slope while for the single-ended mixer measurement we find a slightly negative slope. This effect is a strong evidence for frequency dependent LO noise power. Our assumption is supported by an identical single-ended

mixer measurement, however, using a Gunn driven LO instead of the synthesizer driven LO and which is shown in Fig. 8(d). The slope of the IF is clearly positive which suggests that less near-carrier noise power is produced by this LO compared to the result of Fig. 8(c). This is in agreement with the  $T_{LO}$  value for the LO device used for the measurement shown in Fig. 8(d) which is 38 K and, therefore, in this measurement only 38/2 K additional noise is added to each of the two mixers on the balanced mixer chip. Moreover, we find that the measured single-ended noise performance using the Gunn driven LO is comparable to the balanced mixer measurement shown in Fig. 8(a).

The balanced mixer IF trace has a positive slope because the noise rejection has a certain bandwidth and decreases as a function of  $\nu_{IF}$ . For the measurement shown in Fig. 8(a) the balanced mixer is tuned to have the strongest noise rejection for the small IF frequencies whereas in Fig. 8(c) it is observed that LO noise power has the strongest influence for small values of  $\nu_{IF}$ . This leads to a negative slope of the IF trace which dominates the usually observed increase in the noise temperature for large  $\nu_{IF}$  mainly due to the SIS junction capacitance (Fig. 8(d)). Therefore, the effect of near-carrier noise power should be strongest for small IF frequencies.

#### IV. CONCLUSION AND OUTLOOK

To conclude, we have presented an experimental method which allows to use a balanced mixer as a noise meter. We have shown that as a result of such a measurement the additional noise power contribution of an LO to an astronomical receiver system can be identified. Three LO sources were used in our heterodyne experiment which measured their equivalent noise temperature. The balanced mixer operation provides the measurement of  $T_{rec}$  independent of the noise contribution  $T_{LO}$ . The highest  $T_{LO}$  value was measured for the frequency 460 GHz using the synthesizer driven LO. Components of this LO have low-frequency gain,<sup>28</sup> so that for example even very small low-frequency amplitude noise contributions coming from our synthesizer can result at the end in near-carrier LO noise power, measurable in the IF frequency range 4-8 GHz. An alternative interesting explanation is given by Bryerton *et al.*<sup>8</sup> discussing the possibility of phase noise to amplitude noise conversion in a frequency multiplier chain. If the frequency multiplier chain of the synthesizer driven LO does not significantly contribute to the noise power of the complete LO system<sup>7</sup>, then the power amplifier is the most likely noise source of the LO chain. The large measured difference in  $T_{LO}$  when different power amplifiers were used (PA1 and PA2) indicates this. In this case our measurements can be applied to a THz LO. Attaching the lower frequency active components of a THz LO to our lower frequency LO would provide a measurement method to characterize the THz LO noise performance, rendering precise character-

izations of superconducting THz mixer devices possible. In a heterodyne measurement where we used only one of two mixers on the balanced mixer chip, our measurement shows the impact of LO noise power on single-ended mixers. Here the expected result is that  $T_{LO}$  is added to  $T_{rec}$ . Measuring the receiver noise temperature, the IF trace of a balanced mixer shows a positive slope due to the bandwidth limited noise rejection. Near-carrier LO noise power effects the single-ended IF frequency resolved receiver noise temperature in a different way and the result is an increase of noise at lower frequencies, resulting in an effectively flat or even slightly negative slope. We expect that this effect should significantly decrease the sensitivity of receivers employing HEB mixers, e.g. for frequencies above 1.4 THz where these devices are the heterodyne mixers of choice and where only few balanced mixers were realized to date<sup>29,30</sup>.

## ACKNOWLEDGMENTS

This work is carried out within the Collaborative Research Council 956, sub-project D3, funded by the Deutsche Forschungsgemeinschaft (DFG) and by BMBF, Verbundforschung Astronomie under contract no. 05A08PK2. The excellent support of the in-house machine shop is gratefully acknowledged. M. P. Westig would like to express his gratitude to T. W. Crowe and J. Hesler from Virginia Diodes, Inc., USA, for fruitful discussions and very useful hints concerning the synthesizer driven local oscillator and to J. Childers from Spacek Labs Inc., USA, for a very fast response on questions concerning the power amplifiers. All authors thank the Max-Planck-Institut für Radioastronomie in Bonn, Germany, for the possibility of using their 380-520 GHz synthesizer driven local oscillator source. One of the authors (MPW) would like to thank the Bonn-Cologne Graduate School of Physics and Astronomy for financial and travel support. The balanced mixer devices were fabricated in the KOSMA microfabrication laboratory in Köln.

<sup>1</sup>A. W. Blain, I. Smail, R. J. Ivison, J. -P. Kneib, D. T. Frayer, *Phys. Rep.* **369**, 111 (2002).

<sup>2</sup>J. Zmuidzinas and P. L. Richards, *Proc. IEEE* **92**, 1597 (2004).

<sup>3</sup>C. M. Caves, *Phys. Rev. D* **26**, 1817 (1982).

<sup>4</sup>J. B. Gunn, *Solid State Commun.* **1**, 88 (1963).

<sup>5</sup>Virginia Diodes Inc., Charlottesville, VA, USA. Homepage: <http://www.vadiodes.com>.

<sup>6</sup>J. C. Pearson, B. J. Drouin, A. Maestrini, I. Mehdi, J. Ward, R. H. Lin, S. Yu, J. J. Gill, B. Thomas, C. Lee, G. Chattopadhyay, E. Schlecht, F. W. Maiwald, P. F. Goldsmith, and P. Siegel, *Rev. Sci. Instrum.* **82**, 093105 (2011).

<sup>7</sup>N. Erickson, in *Proceedings of the 15th International Symposium on Space Terahertz Technology* (2004) p. 135.

<sup>8</sup>E. W. Bryerton, M. A. Morgan, D. L. Thacker, and K. S. Saini, in *Proceedings of the 18th International Symposium on Space Terahertz Technology* (2007) p. 68.

<sup>9</sup>E. W. Bryerton and J. Hesler, in *Proceedings of the 19th International Symposium on Space Terahertz Technology* (2008) p. 499.

<sup>10</sup>J. Faist, F. Capasso, D. Sivco, C. Sirtori, A. Hutchinson, and A. Cho, *Science* **264**, 553 (1994).

<sup>11</sup>G. Scalari, D. Turčinková, J. L.- Hughes, M. I. Amanti, M. Fischer, M. Beck, and J. Faist, *Appl. Phys. Lett.* **97**, 081110 (2010).

<sup>12</sup>D. Turčinková, G. Scalari, F. Castellano, M. I. Amanti, M. Beck, and J. Faist, *Appl. Phys. Lett.* **99**, 191104 (2011).

<sup>13</sup>J. C. Bardin and S. Weinreb, *IEEE Microw. Wireless Compon. Lett.* **19**, 407 (2009).

<sup>14</sup>S. Weinreb, J. Bardin, H. Mani and G. Jones, *Rev. Sci. Instrum.* **80**, 044702 (2009).

<sup>15</sup>N. Wadefalk and S. Weinreb, in *Proc. Workshop WFF, IEEE IMS2005 Symp.* (Long Beach, CA, 2005) CD-Rom.

<sup>16</sup>J. J. Freeman, *Principles of Noise* (John Wiley & Sons, Inc., 1958).

<sup>17</sup>K. Rohlfs and T. L. Wilson, *Tools of Radio Astronomy* (Springer, 1999).

<sup>18</sup>M. P. Westig, K. Jacobs, J. Stutzki, M. Justen, and C. E. Honingh, *Supercond. Sci. Technol.* **24**, 085012 (2011).

<sup>19</sup>Our synthesizer is an Agilent Technologies PSG CW signal generator, model number E8247C. The frequency range is 250 kHz - 20 GHz.

<sup>20</sup>The spectrum analyzer used throughout our measurements is of type PXA N9030A with a frequency bandwidth of 3 Hz - 26.5 GHz.

<sup>21</sup>The power amplifiers we use in the synthesizer based local oscillator are from Spacek Labs Inc., Santa Barbara, CA, USA. Homepage: <http://spaceklabs.com>. The amplifier used for the lower frequency channel is of type A369-3XWB-24 and for the higher frequency channel of type A415-3XWB-30.

<sup>22</sup>We use a coupler from ET Industries, model number J-412-180. The frequency bandwidth is 4.0 - 12.4 GHz.

<sup>23</sup>S. A. Maas, *Microwave Mixers* (Artech House, 1986).

<sup>24</sup>J. W. Kooi, A. Kovács, B. Bumble, G. Chattopadhyay, M. L. Edgar, S. Kaye, R. LeDuc, J. Zmuidzinas, and T. G. Philipps, in *Proceedings of SPIE, Millimeter and Submillimeter Detectors for Astronomy II*, Vol. 5498 (2004) p. 332.

<sup>25</sup>J. W. Kooi, R. A. Chamberlin, R. Monje, B. Force, D. Miller, and T. G. Phillips, *IEEE Trans. Terahertz Sci. Technol.* **2**, 71 (2012).

<sup>26</sup>J. R. Tucker and M. J. Feldman, *Rev. Mod. Phys.* **57**, 1055 (1985).

<sup>27</sup>D. Rogovin and D. J. Scalapino, *Ann. Phys.* **86**, 1 (1974).

<sup>28</sup>Private Communication with Jeffrey Hesler, Virginia Diodes, Inc.

<sup>29</sup>D. Meledin, A. Pavolotsky, V. Desmaris, I. Lapkin, C. Risacher, V. Perez, D. Henke, O. Nystrom, E. Sundin, D. Dochev, M. Pantaleev, M. Fredrixon, M. Strandberg, B. Voronov, G. Goltsman, V. Belitsky, *IEEE Trans. Microw. Theory Tech.* **57**, 89 (2009).

<sup>30</sup>D. Dochev, V. Desmaris, D. Meledin, A. Pavolotsky, and V. Belitsky, *J. Infrared Millim. Terahz. Waves* **32**, 451 (2011).